

where

$$P_{N,j}^* = (1/T) \sum_t [X_j(t) - \mu(t)]^2 \quad (j = 1, \dots, J), \quad (\text{A.2})$$

$$\bar{P}_N^* = (1/J) \sum_j P_{N,j}^*, \quad (\text{A.3})$$

$$R = (1/T) \sum_t [\bar{X}(t) - \mu(t)]^2. \quad (\text{A.4})$$

Under the assumptions given in Section II, it can be shown that the variable $J^{1/2}[J/(J-1)]R$ tends in probability to zero as J tends to infinity. Therefore, the asymptotic joint distribution of

$$J^{1/2}(\hat{\sigma}_N^2 - \sigma_N^2) \quad \text{and} \quad J^{1/2}(\hat{\sigma}_X^2 - \sigma_X^2) \quad (\text{A.5})$$

is the same as that of

$$J^{1/2}[\bar{P}_N^* - E(\bar{P}_N^*)] \quad \text{and} \quad J^{1/2}[\bar{P}_X - E(\bar{P}_X)] \quad (\text{A.6})$$

where \bar{P}_X is the average of the variables $P_{X,j}$ defined by (14).

The variables $P_{N,j}^*$ are independent and identically distributed (iid) unbiased estimators of σ_N^2 . Similarly, the variables $P_{X,j}$ are iid unbiased estimators of σ_X^2 . According to the multivariate central limit theorem, the asymptotic joint distribution of the variables given in (A.6) is normal if the variances of $P_{X,j}$ and $P_{N,j}^*$ are finite. These variances are complicated functions that can be expressed as the sum of terms involving the signal power, the noise power, the third and fourth moments of the noise process, and cross product terms of degree less than four. They can be shown to be finite under the assumptions given in Section II.

In order to prove the asymptotic normality of $\hat{S}\hat{N}R$, we write this estimator in the form $\hat{S}\hat{N}R = (\hat{\sigma}_X^2/\hat{\sigma}_N^2) - 1$. Applying a theorem on differentiable functions of asymptotically normal variables [5, ch. 5, theorem 1.9], we have that $J^{1/2}(\hat{S}\hat{N}R - \text{SNR})$ is asymptotically normal with mean zero and variance given by J times (16).

APPENDIX II: ESTIMATION OF $\text{Var}(\hat{\sigma}_X^2)$, $\text{Var}(\hat{\sigma}_N^2)$ AND $\text{Cov}(\hat{\sigma}_X^2, \hat{\sigma}_N^2)$

The unknown variances and covariances in (16) could be estimated by writing down expressions for these parameters in terms of the properties of the signal and noise and replacing unknown quantities by estimates. However, these expressions are very complicated and require estimation of higher order moments of the noise process. A simpler estimation procedure is suggested here.

A natural estimator of the variance of $P_{X,j}$ is

$$[1/(J-1)] \sum_j (P_{X,j} - \bar{P}_X)^2. \quad (\text{A.7})$$

Equation (18) is obtained by noting that $\text{Var}(\hat{\sigma}_X^2) = \text{Var}(P_{X,j})/J$.

Similarly, an estimator of the variance of $P_{N,j}^*$ is

$$[1/(J-1)] \sum_j (P_{N,j}^* - \bar{P}_N^*)^2. \quad (\text{A.8})$$

Because the variables $P_{N,j}^*$ depend on the unknown signal, we substitute $P_{N,j}$ for $P_{N,j}^*$, and obtain (19) by noting that

$$\begin{aligned} \text{Var}(\hat{\sigma}_N^2) &= [J/(J-1)]^2 \text{Var}(\bar{P}_N) \\ &\approx [J/(J-1)]^2 \text{Var}(P_{N,j})/J. \end{aligned} \quad (\text{A.9})$$

The term $J/(J-1)$ can be neglected in the asymptotic argument, but is important in practical applications when J is small.

Equation (20) is obtained in an analogous manner.

REFERENCES

- N. J. Bershad and A. J. Rockmore, "On estimating signal-to-noise ratio using the sample correlation coefficient," *IEEE Trans. Inform. Theory*, vol. IT-20, pp. 112-113, 1974.
- E. Callaway and R. A. Halliday, "Evoked potential variability: Effects of age, amplitude and methods of measurement," *Electroencephalogr. Clin. Neurophysiol.*, vol. 34, pp. 125-133, 1973.
- R. Coppola, R. Tabor, and M. S. Buchsbaum, "Signal to noise ratio and response variability measurements in single trial evoked potentials," *Electroencephalogr. Clin. Neurophysiol.*, vol. 44, pp. 214-222, 1978.
- C. Elberling and M. Don, "Quality estimation of averaged auditory brainstem responses," *Scand. Audiol.*, vol. 13, pp. 187-197, 1984.
- E. L. Lehmann, *Theory of Point Estimation*. New York: Wiley, 1983.
- J. Möcks, T. Gasser, and P. D. Tuan, "Variability of single evoked potentials evaluated by two new statistical tests," *Electroencephalogr. Clin. Neurophysiol.*, vol. 57, pp. 571-580, 1984.
- B. I. Turetsky, J. Raz, and G. Fein, "Noise and signal power and their effects on evoked potential estimation," *Electroencephalogr. Clin. Neurophysiol.*, to be published.

Skin Impedance From 1 Hz to 1 MHz

JAVIER ROSELL, JOSEP COLOMINAS, PERE RIU, RAMON PALLAS-ARENY, AND JOHN G. WEBSTER

Abstract—We measured the impedance of skin coated with gel, but otherwise unprepared from 1 Hz to 1 MHz at ten sites on the thorax, leg, and forehead of ten subjects. For a 1 cm² area, the 1 Hz impedance varied from 10 kΩ to 1 MΩ, which suggests that biopotential amplifier input impedance should be very high to avoid common mode to differential mode voltage conversion. 1 MHz impedance was tightly clustered about 120 Ω. 100 kHz impedance was about 220 Ω, which suggests that the variation in skin impedance may cause errors in two electrode electrical impedance tomographs.

INTRODUCTION

The magnitude of skin impedance is of interest to designers and users of medical instruments. Berson *et al.* [1] measured 10 Hz skin impedance at seven locations on 24 subjects and found values as high as 3.5 MΩ·cm² (larger areas yield lower impedance). Swanson and Webster [2] measured skin impedance on one subject from 1 Hz to 1 MHz and found that for 1 cm², the high impedance at low frequencies decreased to a low value of about 200 Ω at 1 MHz. Abrasion of the skin produced a low impedance over the entire frequency range.

We desired to measure the skin impedance over a large frequency range at a variety of locations on the body. Thus, the results should be applicable when measuring biopotentials such as ECG, EEG, EMG, ENG, EOG, EGG, and in bioimpedance measurements such as electrical impedance plethysmography, impedance cardiography, and electrical impedance tomography.

METHODS

Fig. 1 shows the ten skin sites we tested on each of ten subjects. Others [3] have frequently tested the skin impedance on the ventral forearm because it is a convenient site for a person to measure his own skin impedance. In contrast, Fig. 1 shows that we selected sites typically used when measuring the ECG, impedance plethysmography, impedance cardiography, and electrical impedance tomography. We selected sites that were flat or convex because it

Manuscript received October 9, 1987; revised March 25, 1988. J. G. Webster was supported by the Fulbright Professor/Specialist Exchange Program sponsored by la Caixa, the Fulbright Commission in Madrid, and the United States Information Agency.

J. Rosell, J. Colominas, P. Riu, and R. Pallas-Areny are with the Departamento de Ingeniería Electrónica, División de Instrumentación y Bioingeniería, U.P.C., 08080 Barcelona, Spain.

J. G. Webster is with the Department of Electrical and Computer Engineering, University of Wisconsin-Madison, Madison, WI 53706.

IEEE Log Number 8821505.

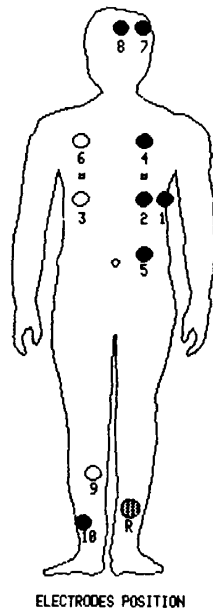


Fig. 1. Electrodes 1, 2, and 3 are at the level of the base of the sternum. Electrode 1 is on the anterior axillary line. Electrodes 2, 4, and 5 are on the midclavicular line. Electrodes 3 and 6 are on the scapular line. Electrode *R* is in the reference electrode.

was difficult to maintain reliable contact with concave sites. The ten subjects were healthy males, aged 19–55 and weights 53–105 kg. Tests were run in Barcelona in July with typical temperatures of 25°C and relative humidity between 60 and 70 percent.

Many electrodes are applied with gel, but without preparing the skin by cleaning or abrasion. Thus to simulate worst case conditions, we used no cleaning or abrasion. This is a critically important method because the slightest abrasion or nicking of the skin during skin preparation will scratch through the barrier layer and drastically lower the low-frequency impedance. This is in contrast with Hary *et al.* [4] who prepared the skin by shaving and cleaning the site with alcohol.

Geddes and Valentinuzzi [5] applied metal electrodes to dry skin. In contrast, we used electrode gel since it is almost universally used with surface electrodes. Like Grimnes [6], we controlled the area wetted by the electrode gel (Parker Spectra 360 Electrode Gel, Orange, NJ 07050) by constructing a plastic cylinder 12.5 mm ID, 15 mm OD, 2.25 mm height with glued-on wings (See Fig. 2(a).) After taping the wings to the skin, we carefully filled the cylinder with gel and applied a Ag/AgCl electrode to the gel. This arrangement enabled us to achieve a constant known area of 0.550 cm² at each location. This would have been impossible by merely applying disposable ECG electrodes because variations in application pressure would have spread the gel over various areas. We corrected all data to an area of 1 cm² by multiplying measured impedances by our current-injecting electrode area of 0.550 cm².

Fig. 2(a) shows an arrangement that includes a special annular electrode we designed to inject current and two different positions for the voltage-measuring electrode (*V*₁, *V*₂). The dashed lines show how the current disperses in the tissue after passing through the skin. The current through the grounded test electrode passes through *Z*_e, *Z*_g, *Z*_s, and *Z*_t [Fig. 2(b)] that are the impedance of the electrode, gel, skin and internal tissues, respectively. Voltage measurements at *V*₁ with respect to ground include the effect of all four of these impedances. Measuring voltage at *V*₂ decreases the effect of *Z*_e because *V*₂ measures the voltage of an isovoltage contour (shown by the solid lines) that is closer to the skin than the

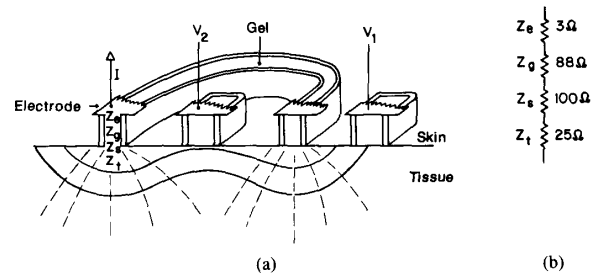


Fig. 2. (a) Current from a distant reference electrode *R* flows through impedances for the electrode *Z*_e, gel *Z*_g, skin *Z*_s, and tissue *Z*_t. Measurements at *V*₁ include all four impedances. Measurements at *V*₂ reduce *Z*_e. (b) Numbers indicate impedances in ohms at 1 MHz. Dashed lines indicate current dispersion. Solid lines indicate isovoltage contours.

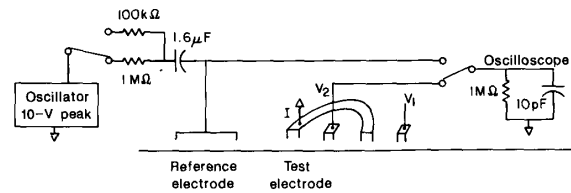


Fig. 3. Current flows from the oscillator through the reference electrode, and then through the test electrode to ground. Impedance is calculated from measurements made at the voltage electrode *V*₂.

isovoltage contour measured by *V*₁. Then we measured *Z*_e + *Z*_g by placing two electrodes face to face. By varying the thickness of gel, we determined separately *Z*_e and *Z*_g. By subtracting *Z*_e + *Z*_g we obtained *Z*_s.

We performed ten measurements on each of ten subjects between 10 and 300 s after gel application. The trend of the impedance measurement changed from site to site for a given person and also depending on the subject. In some cases, repetitive tests at the beginning and ending of the tests at a single location showed no significant change in impedance. However, in other cases we found a decrease of up to 20 percent, which Grimnes [6] attributes to electrolyte penetration. We also found increases of up to 20 percent, which we attribute to closure of the sweat ducts after application of the cool gel. Where we encountered changes of more than 10 percent, we repeated the tests until data were consistent within 10 percent.

Fig. 3 shows the measurement circuit, which is similar to that of Swanson and Webster [2]. Current from a sinusoidal oscillator travels through a large reference ECG plate electrode, then through the test electrode to ground. Since it is difficult to measure the voltage under the skin, we placed the 2 by 5 mm voltage electrode outside the cylinder with a 2 mm spacing of skin to prevent any possible bridging of the gel between electrodes. The 1.6 μF capacitor prevented any dc current from flowing through the skin. To prevent current from affecting the impedance of the skin, currents were 10 μA for frequencies less than 10 kHz, and 100 μA for higher frequencies. We measured voltage values by observing waveforms on an oscilloscope with an estimated error of 5 percent.

RESULTS

Fig. 4 shows the impedance for all data points. The tight clustering of data between 100 kHz and 1 MHz suggests that the high-frequency impedance is nearly the same for all electrode locations and for all subjects. This suggests that the series resistance in the usual three-element model for skin impedance [2] can be fixed at approximately 120 Ω. Between 1 kHz and 100 kHz there is a wider dispersion, which can be modeled by a 10–40 nF capacitor corresponding to the capacitance of the barrier layer to the skin. The

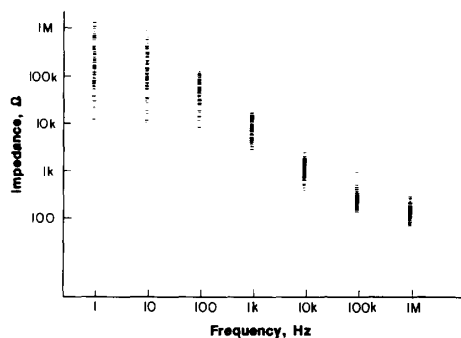


Fig. 4. Impedance versus frequency for all data. High-frequency impedance is about 100 Ω , whereas low-frequency impedance varies from 10 k Ω to 1 M Ω .

much wider variation in the lower-frequency impedance can be modeled by a resistor in parallel with the capacitor. This resistor corresponds to the resistance of the barrier layer of the skin and is easily reduced by any slight abrasion [2].

All of the above results include the sum of the skin and the internal tissue impedance. The effect of Z_i is only important at 1 MHz. By employing the methods described above we were able to estimate the impedance Z_i for the arrangement used as 25 Ω . The numbers shown in Fig. 2(b) give the impedance in ohms of each element at 1 MHz. We note that for our choice of components, the impedance of the gel is comparable to that of the skin. The impedance of the barrier layer is approximately 100 Ω at 1 MHz and suggests that the barrier layer acts as a pure capacitance at high frequencies.

In all subjects, the higher impedance was obtained at sites on the leg, whereas the lower values were those at the forehead. Points 3, 5, and 6 gave a value higher than points 7 and 8, but lower than points 1, 2, and 4.

CONCLUSIONS

Others have noted that the low-frequency impedance of the skin occasionally reaches very high values [1]. This fact requires designers of biopotential amplifiers to achieve extremely high input

impedances over the frequency range of measurement in order to prevent the imbalance in skin impedance from converting common mode voltage to differential voltage.

Our measurements at high frequencies have implications for designers of electrical impedance tomographs. Designers who use a four-electrode system can obtain skin impedance values from Fig. 4 that permit them to determine requirements on current sources and voltage-measuring circuits. Designers who use two-electrode instruments should be particularly careful because measurements with physical phantoms, which do not contain skin, may not yield results similar to measurements that do include skin. Kim and Woo [7] use 100 kHz where the skin impedance is 100 Ω higher than at 1 MHz. Variations in this series impedance cannot be incorporated into the reconstruction algorithm and may produce large distortions in the impedance image. Gisser *et al.* [8] use 12 kHz where the skin impedance is 900 Ω higher than that at 1 MHz, and their problems should be worse.

REFERENCES

- [1] A. S. Berson and H. V. Pipberger, "Skin-electrode impedance problems in electrocardiography," *Amer. Heart J.*, vol. 76, pp. 514-525, 1968.
- [2] D. K. Swanson and J. G. Webster, "A model for skin-electrode impedance," in *Biomedical Electrode Technology*, H. A. Miller and D. C. Harrison, Eds. New York: Academic, 1974, pp. 117-128.
- [3] Y. Yamamoto, T. Yamamoto, and T. Ozawa, "Characteristics of skin admittance for dry electrodes and the measurement of skin moisturisation," *Med. Biol. Eng. Comput.*, vol. 24, pp. 71-77, 1986.
- [4] D. Harry, G. A. Bekey, and D. J. Antonelli, "Circuit models and simulation analysis of electromyographic signal sources—I: The impedance of EMG electrodes," *IEEE Trans. Biomed. Eng.*, vol. BME-34, pp. 91-97, 1987.
- [5] L. A. Geddes and M. E. Valentinuzzi, "Temporal changes in electrode impedance while recording the electrocardiogram with 'dry' electrodes," *Ann. Biomed. Eng.*, vol. 1, pp. 356-367, 1973.
- [6] S. Grimnes, "Impedance measurement of individual skin surface electrodes," *Med. Biol. Eng. Comput.*, vol. 21, pp. 750-755, 1983.
- [7] Y. Kim and H. W. Woo, "A prototype system and reconstruction algorithms for electrical impedance technique in medical body imaging," *Clin. Phys. Physiol. Meas.*, vol. 8, suppl. A, pp. 63-70, 1987.
- [8] D. G. Gisser, D. Isaacson, and J. C. Newell, "Current topics in impedance imaging," *Clin. Phys. Physiol. Meas.*, vol. 8, suppl. A, pp. 39-46, 1987.

Call for Applications for Editor

IEEE TRANSACTIONS ON BIOMEDICAL ENGINEERING

ALL those interested in applying for the Chief Editor's position should send their applications along with their resumes to the President of the IEEE Engineering in Medicine and Biology Society:

Dr. Willis J. Tompkins
Dept. of Electrical & Computer Engineering
University of Wisconsin
1415 Johnson Drive
Madison, WI 53706-1691

Your application should give a brief statement of why you are interested in the position, a statement of your goals, and a description of your qualifications.

The Society expects to fill the position by *January 1989*.

Call For Papers

Special Issue on Laser-Tissue Interaction

TREMENDOUS advances have recently been made in the understanding of the principles underlying the interaction of laser light and tissue. These understandings are leading to the development of unique concepts for treatment and diagnostic devices. The IEEE TRANSACTIONS ON BIOMEDICAL ENGINEERING invites the submission of papers reporting original research in the areas of laser applications in medicine and biology. Areas of interest include, but are not limited to, optics, spectroscopy, heat transfer, rate kinetics, photochemistry, and ablation of tissue. The Guest Editor is Dr. A. J. Welch of the University of Texas at Austin. Papers should be about six transactions pages in length and conform to the format and other limitations set for the TRANSACTIONS. Authors planning to make a contribution are asked to submit a preliminary title and a short abstract. Manuscripts are due by *October 1, 1988*. Please submit all materials to the Guest Editor listed below:

Dr. A. J. Welch
Department of Electrical and Computer Engineering
University of Texas at Austin
Austin, TX 78712
